

Original papers

Deep learning models for plant disease detection and diagnosis

Konstantinos P. Ferentinos

Hellenic Agricultural Organization “Demeter”, Institute of Soil & Water Resources, Dept. of Agricultural Engineering, 61 Dimokratias Av., 13561 Athens, Greece



ARTICLE INFO

Keywords:

Convolutional neural networks
Machine learning
Artificial intelligence
Plant disease identification
Pattern recognition

ABSTRACT

In this paper, convolutional neural network models were developed to perform plant disease detection and diagnosis using simple leaves images of healthy and diseased plants, through deep learning methodologies. Training of the models was performed with the use of an open database of 87,848 images, containing 25 different plants in a set of 58 distinct classes of [plant, disease] combinations, including healthy plants. Several model architectures were trained, with the best performance reaching a 99.53% success rate in identifying the corresponding [plant, disease] combination (or healthy plant). The significantly high success rate makes the model a very useful advisory or early warning tool, and an approach that could be further expanded to support an integrated plant disease identification system to operate in real cultivation conditions.

1. Introduction

Plant disease diagnosis through optical observation of the symptoms on plant leaves, incorporates a significantly high degree of complexity. Due to this complexity and to the large number of cultivated plants and their existing phytopathological problems, even experienced agronomists and plant pathologists often fail to successfully diagnose specific diseases, and are consequently led to mistaken conclusions and treatments. The existence of an automated computational system for the detection and diagnosis of plant diseases, would offer a valuable assistance to the agronomist who is asked to perform such diagnoses through optical observation of leaves of infected plants (Mohanty et al., 2016; Yang and Guo, 2017). If the system was simple to use and easily accessible through a simple mobile application, it could also be a valuable tool for farmers in parts of the world lacking the appropriate infrastructure for the provision of agronomic and phytopathological advice. In addition, in the case of large-scale cultivations, the system could be combined with autonomous agricultural vehicles, to accurately and timely locate phytopathological problems throughout the cultivation field, using continuous image capturing. All these are, of course, valid under the condition that the system could achieve high levels of performance in detecting and diagnosing specific diseases in real-life conditions (i.e., in the cultivation field), and that it could be operated through an appropriate, easy-to-use, and user-friendly mobile application (a first step towards that direction has been made by Johannes et al. (2017) for the specific case of wheat plants).

With the development of computational systems in recent years, and in particular Graphical Processing Units (GPU) embedded processors, Machine Learning-related Artificial Intelligence applications have

achieved exponential growth, leading to the development of novel methodologies and models, which now form a new category, that of Deep Learning (LeCun et al., 2015). Deep learning refers to the use of artificial neural network architectures that contain a quite large number of processing layers, as opposed to “swallower” architectures of more traditional neural network methodologies. The now computationally-feasible deep learning models have revolutionized sectors such as image recognition (LeCun et al., 1998; Dan et al., 2011), voice recognition (Hinton et al., 2012), and other similarly complex processes that deal with the analysis of large volumes of data (LeCun and Bengio, 1995), giving a huge boost to applications that use these processes, like, e.g., self-driving vehicles, machine translation and interpretation, etc. The introduction of these deep learning techniques into agriculture (e.g., Carranza-Rojas et al., 2017), and in particular in the field of plant disease diagnosis (Yang and Guo, 2017), has only begun to take place in the last couple of years, and to a rather limited extent.

The basic deep learning tool used in this work is Convolutional Neural Networks (CNNs) (LeCun et al., 1998). CNNs constitute one of the most powerful techniques for modeling complex processes and performing pattern recognition in applications with large amount of data, like the one of pattern recognition in images. Lee et al. (2015) presented a CNNs system for the automated recognition of plants, based on leaves images. Grinblat et al. (2016) developed a relatively simple, though powerful neural network for the successful identification of three different legume species based on the morphological patterns of leaves' veins. Mohanty et al. (2016) compared two well-known and established architectures of CNNs in the identification of 26 plant diseases, using an open database of leaves images of 14 different plants. Their results were very promising, with success rates in the automated

E-mail address: kp3@cornell.edu.

Table 1a
Information and quantitative data of the database images.

Class	Plant common name	Plant scientific name	Disease common name	Disease scientific name	Images (number)	Laboratory conditions (%)	Field conditions (%)
c_0	Apple	Malus domestica	–	–	1835	89.7	10.3
c_1	Apple	Malus domestica	Apple scab	Venturia inaequalis	630	100.0	0.0
c_2	Apple	Malus domestica	Cedar apple rust	Gymnosporangium juniperi-virginianae	276	100.0	0.0
c_3	Apple	Malus domestica	Black rot	Botryosphaeria obtusa	712	87.2	12.8
c_4	Banana	Musa paradisiaca	–	–	1643	0.0	100.0
c_5	Banana	Musa paradisiaca	Black sigatoka	Mycosphaerella fijensis	240	0.0	100.0
c_6	Banana	Musa paradisiaca	Banana speckle	Mycosphaerella musae	3284	0.0	100.0
c_7	Blueberry	Vaccinium spp.	–	–	1735	86.7	13.3
c_8	Cabbage	Brassica oleracea	–	–	420	0.0	100.0
c_9	Cabbage	Brassica oleracea	Black rot	Xanthomonas campestris	64	0.0	100.0
c_10	Cantaloupe	Cucumis melo	–	–	1055	0.0	100.0
c_11	Cassava (manioc)	Manihot esculenta	Brown leaf spot	Cercosporidium henningsii	43	100.0	0.0
c_12	Cassava (manioc)	Manihot esculenta	Cassava green spider mite	Mononychellus tanajoa & progresivus	892	100.0	0.0
c_13	Celery	Apium graveolens	Early blight, Cercospora	Cercospora apii	1204	0.0	100.0
c_14	Cherry (& sour)	Prunus spp.	–	–	854	100.0	0.0
c_15	Cherry (& sour)	Prunus spp.	Powdery mildew	Podosphaera spp.	1052	100.0	0.0
c_16	Corn (maize)	Zea mays	–	–	4450	26.1	73.9
c_17	Corn (maize)	Zea mays	Cercospora leaf spot	Cercospora zeae-maydis	1457	35.2	64.8
c_18	Corn (maize)	Zea mays	Common rust	Puccinia sorghi	1614	73.9	26.1
c_19	Corn (maize)	Zea mays	Northern Leaf Blight	Exserohilum turcicum	985	100.0	0.0
c_20	Cucumber	Cucumis sativus	–	–	267	0.0	100.0
c_21	Cucumber	Cucumis sativus	Downy mildew	Pseudoperonospora cubensis	1318	0.0	100.0
c_22	Eggplant	Solanum melongena	–	–	515	0.0	100.0
c_23	Gourd	Langenaria spp.	Downy mildew	Pseudoperonospora cubensis	114	0.0	100.0
c_24	Grape	Vitis vinifera	–	–	613	69.0	31.0
c_25	Grape	Vitis vinifera	Black rot	Guignardia bidwellii	1180	100.0	0.0
c_26	Grape	Vitis vinifera	Esca (Black measles)	Phaeomonilla chlamydospora	1384	100.0	0.0
c_27	Grape	Vitis vinifera	Leaf blight	Pseudocercospora vitis	1076	100.0	0.0
c_28	Onion	Allium cepa	–	–	154	0.0	100.0
c_29	Orange	Citrus sinensis	Huanglongbing	Candidatus Liberibacter	5507	100.0	0.0

identification up to 99.35%. However, a main drawback was that the entire photographic material included solely images in experimental (laboratory) setups, not in real conditions in the cultivation field. Sladojevic et al. (2016) developed a similar methodology for plant disease detection through leaves images using a similar amount of data available on the Internet, which included a smaller number of diseases (13) and different plants (5). Success rates of their models were between 91% and 98%, depending on the testing data. More recently, Pawara et al. (2017) compared the performance of some conventional pattern recognition techniques with that of CNN models, in plants identification, using three different databases of (a rather limited number of) images of either entire plants and fruits, or plant leaves, concluding that CNNs drastically outperform conventional methods. Finally, Fuentes et al. (2017) developed CNN models for the detection of 9 different tomato diseases and pests, with satisfactory performance.

In this work, specific CNN architectures were trained and assessed, to form an automated plant disease detection and diagnosis system, based on simple images of leaves of healthy and diseased plants. The available dataset contained images captured in both experimental (laboratory) setups and real cultivation conditions in the field. The proposed deep learning approach may find more general solutions than shallow approaches, which learn with less data but are specific to few crops (e.g., Pantazi et al., 2016). The next section presents the basic principles of the tested models, the datasets used for training and testing, and the experimentations that were designed for the investigation of the factors that affect the performance and robustness of the developed system. Section 3 presents the results of the application of the proposed models for plant disease detection and diagnosis, while the paper closes with some concluding remarks and directions for future research towards the evolution and enhancement of the developed system.

2. Materials and methods

2.1. Convolutional neural network models

Artificial neural networks are mathematical models that mimic the general principles of brain function with their neurons and synapses that interconnect them. Their main characteristic is their ability to be trained through the process of supervised learning. During that process, neural networks are “trained” to model some system with the use of existing data that contain specific matchings of inputs and outputs of the system to be modelled. CNNs (LeCun et al., 1998) are an evolution of traditional artificial neural networks, focused mainly on applications with repeating patterns in different areas of the modeling space, especially image recognition. Their main characteristic is that, with the methodology used in their layering, they drastically reduce the required number of structural elements (number of artificial neurons) in comparison to traditional feedforward neural networks. For image recognition applications, several baseline architectures of CNNs have been developed, which have been successfully applied to complicated tasks of visual imagery.

The five basic CNN architectures that were tested in the problem investigated in this work concerning the identification of plant diseases from images of their leaves, were the following: (i) AlexNet (Krizhevsky et al., 2012), (ii) AlexNetOWTBn (Krizhevsky, 2014), (iii) GoogLeNet (Szegedy et al., 2015), (iv) Overfeat (Sermanet et al., 2013), and (v) VGG (Simonyan and Zisserman, 2014). These models and their training and testing processes, were implemented using Torch7¹ machine learning computational framework, which uses the LuaJIT²

¹ <http://torch.ch>

² <http://www.lua.org>

Table 1b

Information and quantitative data of the database images (continued).

Class	Plant common name	Plant scientific name	Disease common name	Disease scientific name	Images (number)	Laboratory conditions (%)	Field conditions (%)
c_30	Peach	Prunus persica	–	–	360	100.0	0.0
c_31	Peach	Prunus persica	Bacterial sport	Xanthomonas campestris	2297	100.0	0.0
c_32	Pepper, bell	Capsicum annuum	–	–	2029	72.8	27.2
c_33	Pepper, bell	Capsicum annuum	Bacterial spot	Xanthomonas campestris	997	100.0	0.0
c_34	Potato	Solanum tuberosum	–	–	152	100.0	0.0
c_35	Potato	Solanum tuberosum	Late blight	Phytophthora infestans	1000	100.0	0.0
c_36	Potato	Solanum tuberosum	Early blight	Alternaria solani	3167	31.6	68.4
c_37	Pumpkin	Cucurbita spp.	Cucumber mosaic	Cucumber mosaic virus (CMV)	2387	0.0	100.0
c_38	Raspberry	Rubus spp.	–	–	371	100.0	0.0
c_39	Soybean	Glycine max	–	–	6235	81.6	18.4
c_40	Soybean	Glycine max	Downy mildew	Peronospora manshurica	851	0.0	100.0
c_41	Soybean	Glycine max	Frogeye leaf spot	Cercospora sojae	2023	0.0	100.0
c_42	Soybean	Glycine max	Septoria Leaf Blight	Septoria glycines	3565	0.0	100.0
c_43	Squash	Cucurbita spp.	–	–	264	0.0	100.0
c_44	Squash	Cucurbita spp.	Powdery mildew	Erysiphe cichoracearum, Sphaerotheca fuliginea	1835	100.0	0.0
c_45	Strawberry	Fragaria spp.	–	–	456	100.0	0.0
c_46	Strawberry	Fragaria spp.	Leaf scorch	Diplocarpon earlianum	3396	29.7	70.3
c_47	Tomato	Lycopersicon esculentum	–	–	1592	100.0	0.0
c_48	Tomato	Lycopersicon esculentum	Bacterial spot	Xanthomonas campestris pv. Vesicatoria	2127	100.0	0.0
c_49	Tomato	Lycopersicon esculentum	Early blight	Alternaria solani	2579	38.8	61.2
c_50	Tomato	Lycopersicon esculentum	Late blight	Phytophthora infestans	1910	100.0	0.0
c_51	Tomato	Lycopersicon esculentum	Septoria leaf spot	Septoria lycopersici	1771	100.0	0.0
c_52	Tomato	Lycopersicon esculentum	Spider mites	Tetranychus urticae	1653	100.0	0.0
c_53	Tomato	Lycopersicon esculentum	Tomato mosaic virus	Tomato mosaic virus (ToMV)	373	100.0	0.0
c_54	Tomato	Lycopersicon esculentum	Leaf Mold	Fulvia fulva	952	100.0	0.0
c_55	Tomato	Lycopersicon esculentum	Target spot	Corynespora cassiicola	1404	100.0	0.0
c_56	Tomato	Lycopersicon esculentum	TYLCV	Begomovirus (Fam. Geminiviridae)	5357	100.0	0.0
c_57	Watermelon	Citrullus lanatus	–	–	172	0.0	100.0
TOTAL:					87,848	62.7	37.3

programming language. Training algorithms were implemented on the GPU of an NVIDIA® GTX1080 card, using the CUDA® parallel programming platform, in Linux environment (Ubuntu 16.04 LTS operating system).

2.2. Training and testing datasets

An open database containing 87,848 photographs of leaves of healthy and infected plants was used for the training and testing of the CNN models. A preliminary version of the database, containing a smaller number of images, is described in Hughes and Salathé (2015). The database that was used here, includes 58 different classes, where each class is defined as a pair of plant and a corresponding disease, while there are certain classes that contain healthy plants. Tables 1a and 1b presents information on the 58 classes, including some statistical data, such as the number of available images per class, and the percentages of images taken in laboratory setups or in real conditions in cultivation fields. These 58 classes comprise 25 different healthy or diseased plants. As shown in Table 1, more than 1/3 of the available images (37.3%) have been captured in real cultivation conditions in the field. Fig. 1 shows samples of a random class, containing two representative images in laboratory conditions, and two in real conditions. The increased complexity of the latter images is obvious, with several aspects contributing to it, such as multiple leaves and other parts of the plants, irrelevant objects (e.g., shoes), different ground textures, shading effects, etc.

The entire database was initially divided into two datasets, the training set, and the testing set, by randomly splitting the 87,848 images so that 80% of them formed the training set, and 20% formed the testing set. The 80/20 splitting ratio of training/testing datasets is the most commonly used one in neural network applications, and other similar splitting ratios (e.g., 70/30) should not have a significant impact on the performance of the developed models (Fine, 2006). Thus, for the training of the CNN models, 70,300 images were used, while the rest 17,548 images were kept for testing the performance of the models in classifying new, previously “unseen” images. A Python script was developed for the creation of the two datasets, producing uniformly distributed pseudorandom numbers for the random selection of the images, thus the percentages of “laboratory conditions” images and “real conditions” images for both datasets (training and testing) were kept similar to those presented in Table 1. In addition, another approach to the development of the training and testing data was also considered, by pre-processing of the images, which included size reduction and cropping to a 256 × 256 pixels size, while the training/testing ratio was kept the same (80/20). The alternative of using grayscale versions of the images for training was not considered, as previous works (e.g., Mohanty et al., 2016) have indicated that this approach does not improve the final classification performance of deep learning models in similar applications. The same holds for segmentation of the leaves from the background of the images, thus this additional step in the process was also not considered. This holds because deep learning systems like CNNs have the ability to identify the



Fig. 1. Samples of images in laboratory conditions (up) and in field conditions (down) [From class c_49 – Tomato with Early blight]

Table 2
Final CNN training parameters values.

Parameter	Value
Batches/epoch	10,000
Batch size	32
Momentum	0.9
Weight decay	0.0005
Learning rate	0.01–0.0001

important and non-important features of a set of images, and in some way, ignore the latter. Thus, the additional step of segmentation of the objects of interest, which can also become very problematic in complex images like the field-images in the current application, can be avoided.

Finally, a third approach to the separation of the database into training and testing datasets was implemented, focusing on assessing the importance of the type and place of capture of the leaves images, i.e., whether they have been captured in laboratory conditions or in real conditions in the cultivation field. Thus, from the 58 available classes of the form [plant, disease], the 12 which contained images of both types

Table 3
Performance of different CNN model architectures for the identification of [plant, disease] classes on the testing dataset.

Model	Original images				Pre-processed images			
	Success rate	Average error	Epoch	Time (s/epoch)	Success rate	Average error	Epoch	Time (s/epoch)
AlexNet	99.06%	0.0354	47	7034	98.64%	0.0658	50	1022
AlexNetOWTBn	99.44%	0.0192	46	7520	99.07%	0.0332	45	1125
GoogLeNet	97.27%	0.0957	45	7845	97.06%	0.0984	40	2670
Overfeat	98.96%	0.0412	45	6204	98.26%	0.0848	49	1570
VGG	99.48%	0.0223	48	7294	98.87%	0.0542	49	4208

Table 4
Final models' performance on the testing dataset, trained with the original images.

Model	Success rate	Average error	Epoch	Time (s/epoch)
AlexNetOWTBn	99.49%	0.0174	121	6647
VGG	99.53%	0.0223	67	7034

were selected (the rest of the classes solely consist either of laboratory conditions images or field conditions images, as shown in Table 1). With these 12 classes, two experiments were conducted and two CNN models were developed, respectively: one which was trained with solely laboratory conditions images and tested on field conditions images, and another which was trained and tested reversely, i.e. it was trained with field conditions images and tested on laboratory conditions images. In both cases, the training/testing ratio was not ideal, because, in those 12 classes, the percentage of laboratory conditions images was 55.8% and of field conditions images was 44.2%, thus the training/testing ratio was far from the 80/20 ratio that was used in the development of the basic model. In the second case in particular, the training set was smaller than the testing set, something that, in general, is not acceptable. However, the results, as presented in the following section, are quite indicative.

3. Results

3.1. Optimal deep learning model

All different CNN models presented in Section 2.1 were trained using the training parameters shown in Table 2. After appropriate experimentation, these values gave the best results during training. The learning rate followed a specific annealing schedule, starting from 0.01 and descending every 20 epochs by 1/2 or by 1/5, alternately, down to 0.0001. Comparison of the models was based on their performance on the testing set (all models achieved 100% accuracy on the training set). Table 3 presents successful classification percentages during testing of the various models, for the two basic training/testing approaches of the 58 classes (i.e., training/testing in a 80/20 ratio, with the original images in the first case, and the pre-processed, down-scaled, squared images in the second case). Presented metrics include:

- the percentages of successful classification of [plant, disease] classes: this is the number of correctly classified images over the total number of images, where “classification” is the first choice of the models, meaning that the successful classification is the opposite of the top-1 error,
- the corresponding average errors of the models: this is the average losses per batch, over all batches of the testing set,
- the training epoch at which best performances were achieved,
- the average time per epoch (in seconds) required for the training of each model.

The results presented in Table 3 indicate that all models achieve better performance when using the original plant leaves images, with

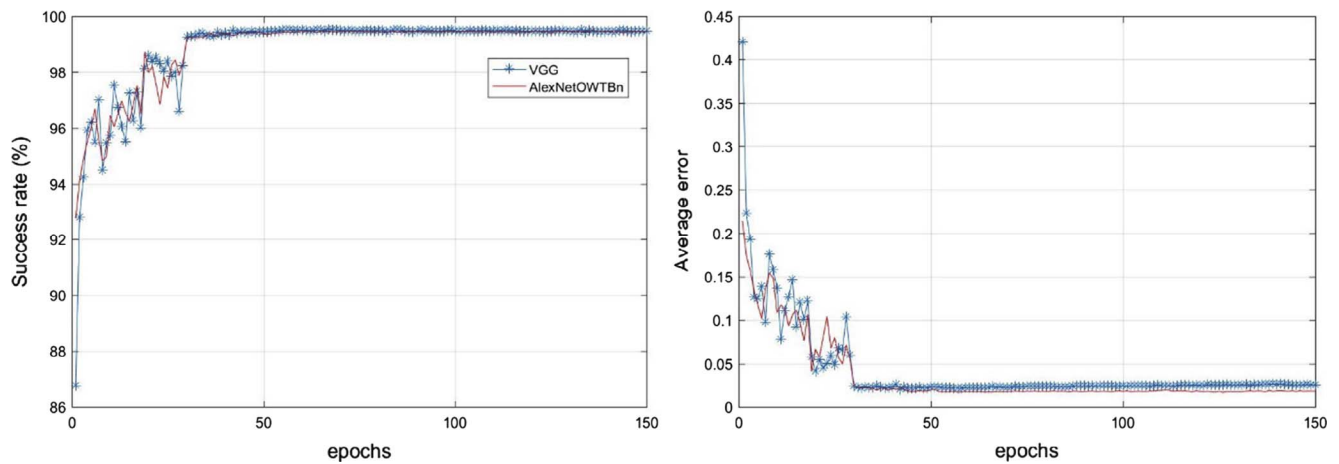


Fig. 2. Success rates and average errors of the final models on the testing dataset, during training.

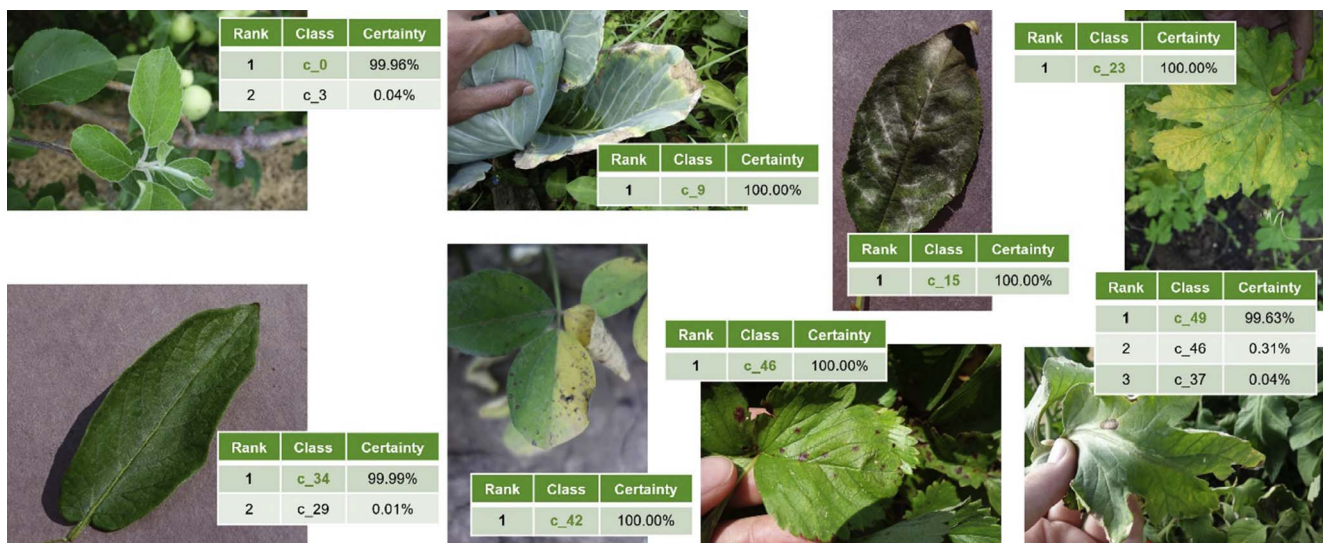


Fig. 3. Examples of correct classifications of various images of the testing dataset.

Table 5

Final models' performance with different training/testing scenarios in respect to laboratory-conditions and field-conditions images.

Model	Training: Laboratory - Testing: Field				Training: Field - Testing: Laboratory			
	Success rate	Average error	Epoch	Time (s/epoch)	Success rate	Average error	Epoch	Time (s/epoch)
AlexNetOWTBn	32.23%	3.5484	53	4375	62.57%	1.9369	104	–
VGG	33.27%	7.8541	54	4901	65.69%	2.6786	134	–

the inevitable consequence of requiring more training time. The highest success rates were achieved by the VGG (highest success rate) and AlexNetOWTBn architectures (lowest final average testing error). These two models were further trained, using solely the original images, for a larger number of training epochs. As shown in Table 4, the final highest successful classification percentage of 99.53% (i.e., a top-1 error of 0.47%) was achieved by the VGG model, which constituted the final model of plant disease detection. Total training time for that model was about 5.5 days (on a single GPU, as described in Section 2.1). Fig. 2 presents the performance on the testing dataset for both models, during their training process. Fig. 3 shows some classification cases of randomly selected images throughout the testing dataset. Classification of an image takes on average about 2 ms on the same GPU that was used for training. Classification results on the tables next to each image are sorted based on the certainty level of each output class (the class with

the highest certainty level (i.e., Rank 1) is considered to be the final outcome of the model's prediction). All images shown in Fig. 3 were correctly classified, i.e., their corresponding classes were those returned with the highest certainty by the model (Rank 1). In most cases, no actual ranking exists, as the correct classification was returned with a certainty level of about 100%.

3.2. Importance of training images type

The two most successful CNN models (VGG and AlexNetOWTBn) were further tested for the investigation of the importance of training images capturing type, as analyzed in Section 2.2. The corresponding results are presented in Table 5. As expected, success rates are significantly lower than those achieved by using a combination of laboratory and field conditions images, despite the smaller number of

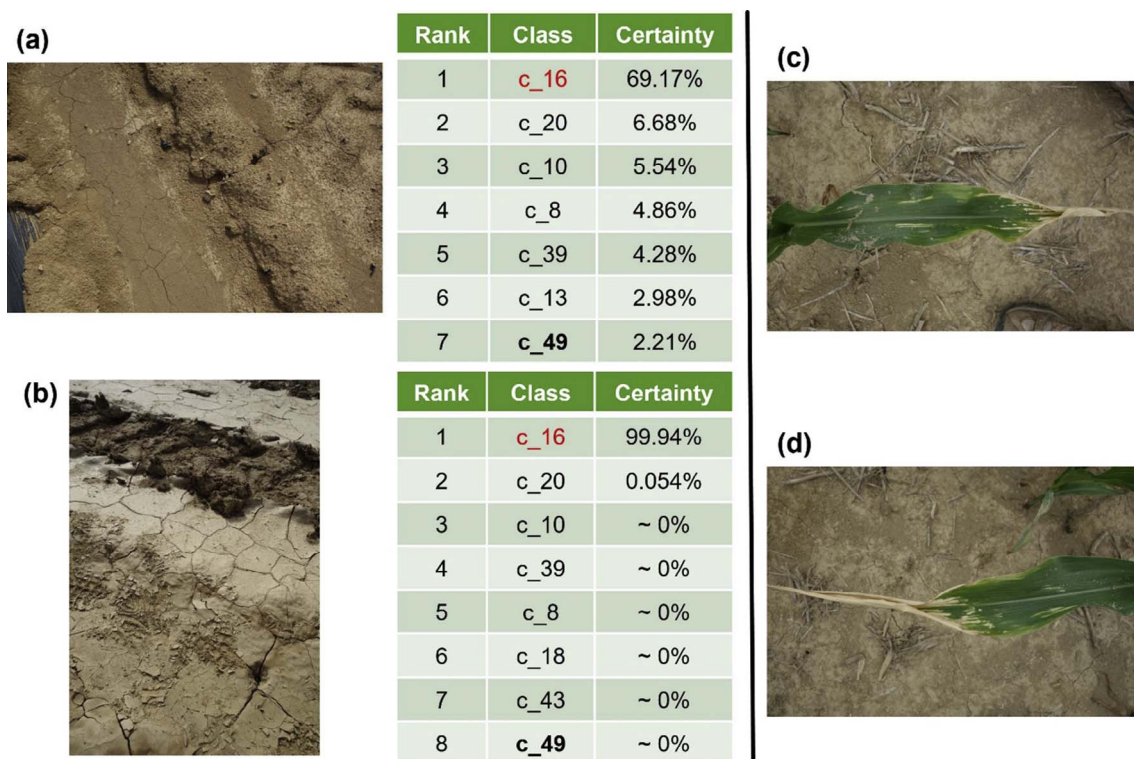


Fig. 4. (a) and (b): Faulty images registered in class c_49 and their corresponding “classification” results. (c) and (d): Representative images of class c_16, “explaining” the classification results of (a) and (b).

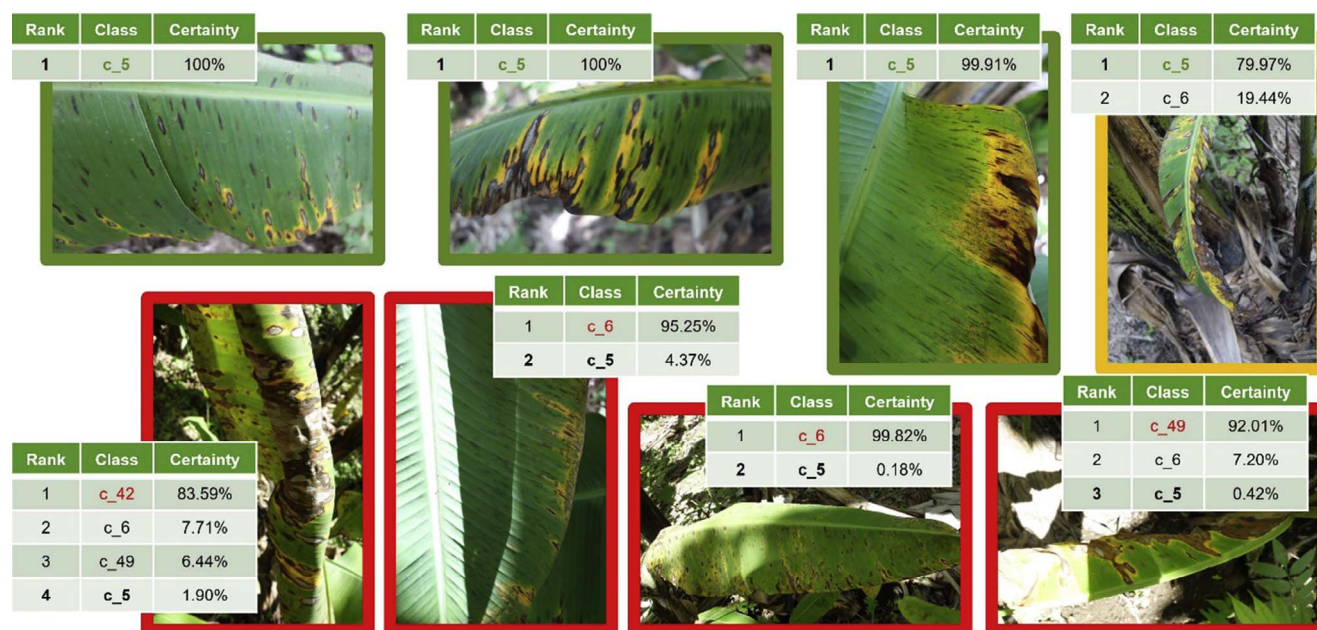


Fig. 5. Representative examples of correct (green and yellow rectangles) and incorrect (red rectangles) classifications of testing images of the class c_5 (Banana with Black sigatoka). (For interpretation of the references to colour in this figure legend, the reader is referred to the web version of this article.)

available classes in the classification process (12 instead of 58). The results show that models achieve better performance when trained with field-conditions images and asked to identify laboratory-conditions images (success rates up to almost 68%). On the other hand, when trained solely on laboratory-conditions images and asked to identify field-conditions images, success rates are significantly lower (about 33%). This demonstrates the fact that image identification in actual cultivation conditions is a much more difficult and complex task than in the case of laboratory-conditions images, and proves the high

importance of the existence of images captured in actual cultivation conditions for the development of useful and successful systems for the automated detection and diagnosis of plant diseases.

3.3. Problematic situations and indicative cases

The success rate of 99.53% that the final model achieved on the testing dataset of 17,548 images, corresponds to correct classification of 17,466 images, i.e., the CNN model did not identify correctly the classes

([plant, disease] combinations) of just 82 images (0.47%). Among these 82 misclassified images, there were some few “faulty” ones that contained no plant leaves at all, like for example, those shown in Fig. 4(a) and (b). In that specific case, the “faulty” images were registered in class c_49 of the database (Tomato with Early blight), while the model classified them in class c_16 (healthy Corn), as shown on the classification tables in Fig. 4. These tables present the ranked outputs of the final CNN model for the images on their left. These images were counted as misclassifications in the performance estimation of the model (a “correct” classification would be the class c_49, even though they do not actually belong to any class, as they do not contain any plant leaves). They were both classified as class c_16 probably due to the fact that the images of that class (two representative ones are shown in Fig. 4(c) and (d)) contained mainly similar soil texture and the corn leaves were very slim, occupying a rather small portion of the image. Thus, the actual accuracy of the final model, if such examples were excluded, would be even higher than 99.53%.

Other problematic situations regarding the field-conditions images of the database included: (i) images with extensive partial shading on the leaves, (ii) images with multiple objects in addition to the pictured leave or leaves, such as fingers, entire hands, shoes, parts of shirts, etc., and (iii) images with the leave occupying a very small and non-centric part of the frame. Judging from the high performance of the final model, these problems were overcome by the learning process in most cases. An indicative case was that of class c_5 (Banana with Black sigatoka), where 4 out of a total of 48 testing images were mistakenly classified (i.e., misclassification reached 8.33%, in contrast to the overall misclassification rate of 0.47%). Fig. 5 shows the classification results of the model on 8 representative images of the c_5 class, including the 4 misclassified ones (inside red rectangles). The first three images inside green rectangles were classified correctly with a certainty of practically 100%, while the image inside the yellow rectangle was classified correctly with a certainty of about 80% (the second choice with a certainty level of 19.4% was class c_6, which corresponds to banana plant with a different disease). The 4 misclassified images (in the red rectangles) suffered mainly from extensive partial shading effects, which probably confused the CNN model, even though in two of them, the correct classification was the second choice of the model, with the first choice being the similar class c_6 (Banana plants with banana speckle disease), thus the model identified correctly the plant species but did not accurately detected the existing plant disease.

4. Conclusions

In this work, specialized deep learning models were developed, based on specific convolutional neural networks architectures, for the identification of plant diseases through simple leaves images of healthy or diseased plants. The training of the models was performed using an openly available database of 87,848 photographs, taken in both laboratory conditions and real conditions in cultivation fields. The data comprises 25 plant species in 58 distinct classes of [plant, disease] combinations, including some healthy plants. The most successful model architecture, a VGG convolutional neural network, achieved a success rate of 99.53% (top-1 error of 0.47%) in the classification of 17,548 previously unseen by the model plant leaves images (testing set). Based on that high level of performance, it becomes evident that convolutional neural networks are highly suitable for the automated detection and diagnosis of plant diseases through the analysis of simple leaves images. In addition, the high importance of the existence of real-conditions images (captured in the cultivation fields) in the training data, which was indicated by the presented results, suggests that, in the development of such models, focus should be given in the maximization of the ratio of real-conditions images in the training data. Furthermore, the low computational power required by the trained model to classify a given image (about 2 ms on a single GPU), makes feasible its integration into mobile applications for their use in mobile devices. Such

devices could be either smartphones, to be used by growers or agronomists, or drones and other autonomous agricultural vehicles, to be used for real-time monitoring and dynamic disease detection on large-scale open-field cultivations. In the former case in particular, except for the fact that a farmer at a remote location could have an incipient warning about a possible threat for his/her cultivation, and an agronomist could have a valuable advisory tool in his/her disposal, a future possibility could be the development of an automated pesticide prescription system that would require a confirmation by the automated disease diagnosis system to allow the purchase of appropriate pesticides by the farmers. That would drastically limit the uncontrolled acquisition of pesticides that leads to their overuse and misuse, with the consequent catastrophic effects on the environment.

Despite the significantly high success rate of the developed system, there are various reasons that make it still quite far from being a generic tool that could be used in real conditions. The inclusion of 58 different classes of [plant, disease] combinations of 25 different plant species constitutes, to our knowledge, the largest plant disease identification task tackled with deep learning methodologies at the moment. However, the expansion of the existing database to incorporate a wider variety of plant species and diseases should be the next immediate future step, a process that can be challenging in several aspects, as well as time demanding. Another important issue that should be noted and should be resolved, is that the testing dataset used for the assessment of the models, was part of the same database that constituted the training set. This is common practice in machine learning models, but the real value of the developed system, especially for being able to be used in real situations, should be proven in testing data that would come from various different sources and/or databases. Some preliminary experiments towards that direction, in a limited however amount of data, showed a substantial reduction in model performance, in the range of 25–35%, depending on the data source, which is similar to corresponding performances reported in the literature (e.g., Mohanty et al. (2016) reported a model accuracy of 31% in such data, for a problem with 38 plant disease classes). For an improvement towards that direction, a much wider variety of training data should be collected, from several sources of different geographic areas, cultivation conditions, and image capturing modes and sets. The proposed deep learning approach showed its high potential, thus it is a matter of quantity and quality of available data to improve the system, and make it wider (in terms of plant species and diseases that can be identified) and more robust in real cultivation conditions.

References

- Carranza-Rojas, J., Goeau, H., Bonnet, P., Mata-Montero, E., Joly, A., 2017. Going deeper in the automated identification of Herbarium specimens. *BMC Evol. Biol.* <http://dx.doi.org/10.1186/s12862-017-1014-z>.
- Dan, C., Meier, U., Masci, J., Gambardella, L.M., Schmidhuber, J., 2011. Flexible, high performance convolutional neural networks for image classification. *Proceedings of the 22nd International Joint Conference on Artificial Intelligence*, vol. 2, pp. 1237–1242.
- Fine, T.L., 2006. *Feedforward Neural Network Methodology*. Springer Science Business Media.
- Fuentes, A., Yoon, S., Kim, S.C., Park, D.S., 2017. A robust deep-learning-based detector for real-time tomato plant diseases and pest recognition. *Sensors* 17, 2022. <http://dx.doi.org/10.3390/s17092022>.
- Grinblat, G.L., Uzal, L.C., Larese, M.G., Granitto, P.M., 2016. Deep learning for plant identification using vein morphological patterns. *Comput. Electron. Agric.* 127, 418–424.
- Hinton, G., Deng, L., Yu, D., Dahl, G.E., Mohamed, A.R., Jaitly, N., Senior, A., et al., 2012. Deep neural networks for acoustic modeling in speech recognition: The shared views of four research groups. *IEEE Signal Process. Mag.* 29 (6), 82–97.
- Hughes, D.P., Salathé, M., 2015. An open access repository of images on plant health to enable the development of mobile disease diagnostics. *arXiv:1511.08060*.
- Johannes, A., Picon, A., Alvarez-Gila, A., Echazarra, J., Rodríguez-Vaamonde, S., Navajas, A.D., Ortiz-Barredo, A., 2017. Automatic plant disease diagnosis using mobile capture devices, applied on a wheat use case. *Comput. Electron. Agric.* 138, 200–209.
- Krizhevsky, A., 2014. One weird trick for parallelizing convolutional neural networks. *arXiv:1404.5997*.
- Krizhevsky, A., Sutskever, I., Hinton, G.E., 2012. Imagenet classification with deep convolutional neural networks. In: *Advances in Neural Information Processing Systems*,

- Eds. F. Pereira, C.J.C. Burges, L. Bottou, and K.Q. Weinberger (Curran Associates, Inc.), pp. 1097–1105.
- LeCun, Y., Bengio, Y. 1995. Convolutional networks for images, speech, and time series. In: *The handbook of brain theory and neural networks*, vol. 3361(10).
- LeCun, Y., Bengio, Y., Hinton, G., 2015. Deep learning. *Nature* 521, 436–444. <http://dx.doi.org/10.1038/nature14539>.
- LeCun, Y., Bottou, L., Bengio, Y., Haffner, P., 1998. Gradient-based learning applied to document recognition. *Proc. IEEE* 86 (11), 2278–2324.
- Lee, S.H., Chan, C.S., Wilkin, P., Remagnino, P. 2015. Deep-plant: Plant identification with convolutional neural networks. 2015 IEEE Intl Conf. on Image Processing, pp. 452–456.
- Mohanty, S.P., Hughes, D.P., Salathé, M., 2016. Using deep learning for image-based plant disease detection. *Front. Plant Sci.* 7 <http://dx.doi.org/10.3389/fpls.2016.01419>. Article: 1419.
- Pantazi, X.E., Moshou, D., Tamouridou, A.A., Kasderidis, S. 2016. Leaf disease recognition in vine plants based on local binary patterns and one class support vector machines. 12th IFIP International Conference on Artificial Intelligence Applications and Innovations (AIAI 2016), Sept. 16–18, Thessaloniki Greece, Proceedings, Springer, pp. 319–327.
- Pawara, P., Okafor, E., Surinta, O., Schomaker, L., Wiering, M. 2017. Comparing local descriptors and bags of visual words to deep convolutional neural networks for plant recognition. 6th Intl Conf. on Pattern Recognition Applications and Methods (ICPRAM 2017).
- Sermanet, P., Eigen, D., Zhang, X., Mathieu, M., Fergus, R., & LeCun, Y. 2013. Overfeat: Integrated recognition, localization and detection using convolutional networks. arXiv:1312.6229.
- Simonyan, K., Zisserman, A. 2014. Very deep convolutional networks for large-scale image recognition. arXiv:1409.1556.
- Sladojevic, S., Arsenovic, M., Anderla, A., Culibrk, D., Stefanovic, D., 2016. Deep neural networks based recognition of plant diseases by leaf image classification. *Computat. Intelligence Neurosci.* <http://dx.doi.org/10.1155/2016/3289801>. Article ID: 3289801.
- Szegedy, C., Liu, W., Jia, Y., Sermanet, P., Reed, S., Anguelov, D., et al. 2015. Going deeper with convolutions. *Proc. of the IEEE Conference on Computer Vision and Pattern Recognition*.
- Yang, X., Guo, T., 2017. Machine learning in plant disease research. *Europ. J. BioMed. Res.* 6–9. <http://dx.doi.org/10.18088/ejbmr.3.1.2016.pp6-9>.